Solid Freeform Fabrication 2021: Proceedings of the 32nd Annual International Solid Freeform Fabrication Symposium – An Additive Manufacturing Conference
Reviewed Paper

A PERIODIC HOMOGENIZATION MODEL INCLUDING POROSITY TO PREDICT ELASTIC PROPERTIES OF 3D-PRINTED CONTINUOUS CARBON FIBER-REINFORCED COMPOSITES

V. Marchal, F. Peyraut*, Y. Zhang, N. Labed

ICB, UMR 6303, CNRS, Université Bourgogne Franche-Comté, UTBM, F-90010 Belfort France

ABSTRACT

Adding continuous carbon fiber into the Fused Filament Fabrication (FFF) process is critical to get reinforced composite structures with improved mechanical properties. However, it remains difficult for the designer to create optimized complex composite structures. Indeed, performing numerical simulations on these materials require to know their elastic coefficients, which are difficult to determine. Using a model of periodic homogenization which considers both the fiber content and the porosity, would be a quick solution to predict the mechanical properties of the printed composite. Based on material studies and validated mechanical tests, this simulation model allows the use of a homogeneous material to replace the composite material for the finite element analysis. This will greatly reduce the number of elements required in the model, leading to a big decrease of the computation cost. Hence, the numerical model has potential to perform simulation-driven design processes, such as generative design.

Keywords: Continuous fiber printing, periodic homogenization, elastic properties

1. INTRODUCTION

The development of additive manufacturing in the last four decades has led to the creation of several techniques, such as Fused Filament Fabrication (FFF), Selective Laser Sintering (SLS), Direct ink Writing (DiW), Stereolithography (SLA), Laminated Object Manufacturing (LOM) and Electron Beam Melting (EBM) [1-3]. The most widely used technique is the FFF, also known as Fused Deposition Modeling (FdM) [3-7]. Its main advantages compared to traditional plastic manufacturing processes (injection, thermoforming, etc.) are the cost-efficiency and the minimal waste of raw material in a lifecycle view [5-7]. Moreover, it is easy to automatize and do not require any other tool except for the printer [6, 8]. Yet, it is mainly used for prototyping, as it results in bad mechanical properties [3, 7].

One way to obtain better properties is to work with composite materials. There are two kinds of reinforcement compatible with the FFF process: short fibers and continuous fibers [1-9]. Short-fiber reinforced composites have a small increase of both mechanical and thermal properties comparing to pure matrix polymers. Ning et al. [10] estimated an increase of 31.6% of the Young's modulus and 22% of the tensile resistance by adding short carbon fibers in an ABS matrix. Moreover, the carbon fibers reduce the thermal expansion [2, 6], which leads to a better printing accuracy. However, short fibers-reinforced composites' properties remain bad comparing to metal alloys. To gain more improvement of the mechanical properties, continuous fibers reinforcement was developed [3-9]. Yet, the additive manufacturing of these materials is not easy because it is difficult to obtain a good bond between the thermoplastic matrix and the

* Corresponding author.
E-mail address: francois.peyraut@utbm.fr

fibers [2, 8]. Recently, some commercial machines were released that reported components with similar stiffness to Aluminum alloys [11]. Such performances could open a wide range of applications for additive manufacturing, especially for complex composite components. However, there is no design support tool tailored for this kind of process, which may form barrier to its application. One key reason is that there is no accurate numerical tool to conduct mechanical simulation and optimization. The manufacturing constraints, such as minimum overhang angle, minimum hole diameter, minimum post diameter or minimum engraved feature size [4], and structure performance are hard to simulate for this process. To build a simulation model, the composite material properties must be precisely characterized.

Several methods are used to predict the elastic properties of a continuous fiber-reinforced composite. For traditional composites, the most used one is the Rule of Mixtures (RoM), which can precisely predict the properties of the material thank to the properties of the fiber, the properties of the matrix and the fiber's content. So, Polyzos et al. [5] had tested several RoMs methods and had compared them with the experimental results of Pyl et al. [12]. The results are accurate in the fiber's direction with all methods. Yet, there is a gap between RoMs results and tests results in the transverse direction to the fiber. To fill this gap, an alternative to RoMs for predicting the properties of heterogeneous materials is to use the periodic homogenization method [13-16]. Dutra et al. [17] applied this method to 3D-printed continuous fiber-reinforced composites and stuck with experimental values in the transversal direction. They increased in their models the stiffness value of the thermoplastic resin to obtain a fair agreement between experimental and numerical results. In this paper, we propose to account for the porosity in our model to predict properly the behavior of a continuous carbon fiber-reinforced 3D-printed composite.

This paper is organized as follows: Section 2 explains the development of the periodic homogenization model; Section 3 validates this model with real tests and the last section concludes the work.

2. PERIODIC HOMOGENIZATION MODEL

As the rule of mixtures gives a poor accuracy in the transverse direction, the periodic homogenization method was selected to predict the elastic properties of the continuous carbon fiber-reinforced material. This method was introduced in the 1970s for modelling the behavior of composite structures with a periodic arrangement of matter [13-16]. It met a great success alongside the emergence of the finite element method and was recently used in the context of additive manufacturing by Dutra et al. [17]. The periodic homogenization method assumes the existence of a two-scales asymptotic expansion of the displacement field $\boldsymbol{u}$:

$$\boldsymbol{u} = \boldsymbol{u}_0(\boldsymbol{x},\boldsymbol{y}) + \varepsilon\, \boldsymbol{u}_1(\boldsymbol{x},\boldsymbol{y}) + \varepsilon^2\, \boldsymbol{u}_2(\boldsymbol{x},\boldsymbol{y}) + \cdots;\ \boldsymbol{y} = \frac{\boldsymbol{x}}{\varepsilon} \tag{1}$$

where $\boldsymbol{x}$ and $\boldsymbol{y}$ represent the macroscopic and microscopic coordinates, respectively. The small parameter ε describes the relative size of the representative unit cell compared to the length of the whole structure. Based on the assumption of eq. (1), it is well-known [16] that the homogenized elastic modulus A_{ijkl} are defined by:

$$A_{ijkl} = \frac{1}{|Y|}\iiint_Y \left(a_{ijkl}(\boldsymbol{y}) - a_{ijpq}(\boldsymbol{y})\frac{\partial \chi_p^{kl}(\boldsymbol{y})}{\partial y_q}\right) dY, \tag{2}$$

where *Y* represents the unit cell, $|Y|$ its volume, a_{ijkl} are the elastic modulus of each constituent embedded in the unit cell (the index *i*, *j*, *k* and *l* vary from 1 to 3), and $\boldsymbol{\chi}^{kl}(\boldsymbol{y})$ are the unknown *Y*-periodic functions solution of the following variational problem:

$$\iiint_Y a_{ijpq}(\boldsymbol{y}) \frac{\partial \chi_p^{kl}(\boldsymbol{y})}{\partial y_q} \frac{\partial v_i(\boldsymbol{y})}{\partial y_j} dY = \iiint_Y a_{ijkl}(\boldsymbol{y}) \frac{\partial (\boldsymbol{\chi^0})_p^{kl}(\boldsymbol{y})}{\partial y_q} \frac{\partial v_i(\boldsymbol{y})}{\partial y_j} dY \quad \forall \boldsymbol{v}\ Y-\text{periodic} \tag{3}$$

$$(\boldsymbol{\chi^0})^{kl} = \frac{1}{2}(y_k \boldsymbol{e_l} + y_l \boldsymbol{e_k});\ \boldsymbol{e_1} = \begin{Bmatrix} 1 \\ 0 \\ 0 \end{Bmatrix};\ \boldsymbol{e_2} = \begin{Bmatrix} 0 \\ 1 \\ 0 \end{Bmatrix};\ \boldsymbol{e_3} = \begin{Bmatrix} 0 \\ 0 \\ 1 \end{Bmatrix} \tag{4}$$

Note that we have adopted in eq. (3) the Einstein convention upon the repeated index. Also note that finding the solutions of eq. (3) consists in solving 6 problems because there are 6 possible combinations for (k,l): $(1,1), (2,2), (3,3), (1,2), (1,3)$ or $(2,3)$. Moreover, if the strategy of developing an in-house code is not retained, a specific computational approach must be adopted because the right-hand side of eq. (3) does not correspond to a standard loading. In this context, a specific approach linked to "black box" commercial FE software was proposed by Cheng et al. [18]. This approach consists in finding an equivalent formulation of (3)-(4) that is compatible with the classical loadings and boundary conditions resources provided by commercial software tools. It was especially demonstrated in [18] that solving eq. (3) was rigorously equivalent to applying the following 3 steps:

- Step 1: Apply (4) as restrained conditions on all the nodes of the mesh. Solve a standard elastic problem on the unit cell without periodic conditions. Get the reaction solution $\boldsymbol{f}^0$ after the FE computation.
- Step 2: Apply the reaction solution $\boldsymbol{f}^0$ obtained in Step 1 as an input of this step. Solve a standard elastic problem on the unit cell with periodic conditions. Get the nodal displacement $\boldsymbol{U}$ after the FE computation.
- Step 3: Apply the nodal displacement $\boldsymbol{U}$ obtained in Step 2 as an input of this step. Solve a standard elastic problem on the unit cell without periodic conditions. Get the reaction solution $\boldsymbol{f}$ after the FE computation.

Each step requires 6 computations, and 36 FE calculations are needed in total. The results of these calculations are combined by considering the contribution of each node of the mesh, yielding to the following expression of the homogenized elastic modulus:

$$A_{ijkl} = \sum_{n=1}^{N} \left((\boldsymbol{\chi^0})^{ij} - \boldsymbol{U}^{ij}\right)_n ((\boldsymbol{f})^{kl} - (\boldsymbol{f^0})^{kl})_n, \tag{5}$$

where *N* represents the number of nodes of the unit cell mesh. Many technical details are presented in [19] if this approach is used with the commercial Abaqus code. We have implemented it with the APDL programming resource (Ansys Parametric Design Language) of the commercial Ansys code.

2.1. Unit Cell

As the periodic homogenization method uses the periodic aspect of the composite material, a unit cell which repeats itself in space is considered (Figure 1).

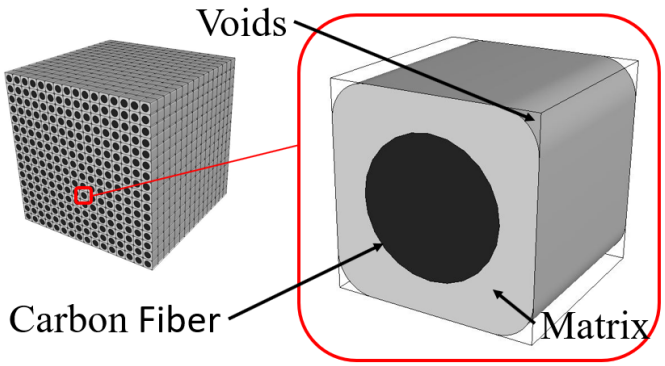

***Figure 1**-Unit cell extracted from the whole structure.*

2.1.1. Determination of the fiber volume content

The fiber content is the most critical parameter of the unit cell. Indeed, the fiber is around two hundred times stiffer than the matrix, so the proportions of the two materials inside the composite have an important influence on the homogenized elastic constants. There are two major methods to determine the fiber content. The first one is the microscope analysis, where we observe a section perpendicular to the fiber and measures the fibers area compared to the total section's area [9, 12, 20-22]. The second one is the degradation of the matrix (with chemical or thermal methods), where we weight a composite part and makes the matrix disappear to get the fibers only. By weighting the fibers and comparing it to the initial mass, we can obtain the mass content of fibers [17, 23]. Table 1 summarizes results, obtained for unidirectional parts printed by Markforged printers, from the literature:

Reference	Printer	Method	Fiber Volume Rate
Blok et al. [9]	Markforged MarkOne	Optical microscope analysis on printed part	27%
Pyl et al. [12]	Markforged MarkTwo	Electron microscope analysis on printed part	27%
Dutra et al. [17]	Markforged MarkOne	Burn-off test (ASTM D3171-15)	32.8%
Chabaud et al. [20]	Markforged MarkTwo	Optical microscope analysis on the filament	35%
Fernandes et al. [21]	Markforged MarkTwo	Optical microscope analysis on printed part	30%
Ekoi et al. [22]	Markforged MarkTwo	Electron microscope analysis on printed part	36.8%
van der Klift et al. [23]	Markforged MarkOne	Matrix Degradation	34.5%

***Table 1** - Literature review about the fiber volume content.*

The fiber volume contents of all studies are in a range between 27% and around 37%. To estimate this rate, we performed a Thermogravimetric Analysis (TGA) on a printed part. This method is close to the one used by Dutra et al. [17] and van der Klift et al. [23]. We obtained a fiber mass content of 44.5%, which gives a fiber volume content of 33.7%. This result is of the same order of magnitude as that reported in the literature and will be used as input of the proposed periodic homogenization model.

2.1.2. Determination of porosity value for modeling

The second required data to size the dimension of the unit cell is the porosity. Blok et al. [9] characterized three kinds of porosities of a 3D printed continuous fiber-reinforced composite: inter-bead voids, fiber pull-outs and gas bubbles. As the characterization on porosity is out of the scope of this paper, to illustrate the modeling, we adopted the porosity values reported in literature (Table 2) to design our unit cell. It is noted that the porosity varies between 7% and 15%. To study the influence of this porosity on the homogenized elastic properties, a parametric study on the unit cell is performed in section 3.3.

Reference	Printer	Method	Porosity
Melenka et al. [3]	Markforged MarkOne	Unknown	10%
Blok et al. [9]	Markforged MarkOne	Unknown	9%
Chabaud et al. [20]	Markforged MarkTwo	Dry-Wet method (ASTM D2734-16)	15%
Ekoi et al. [22]	Markforged MarkTwo	Electron Microscope Analysis	7-11%

Table 2 - *Porosity value range reported in literature.*

2.2. Inputs for the periodic homogenization model

Our unit cell contains two materials, the fiber and the matrix, marked respectively in blue and purple in Figure 2. The fiber content was selected to be 33.7% according to section 2.1.1. For the matrix, we used a linear isotropic material with a Young's modulus of 1.7 GPa (Nylon properties from the Markforged Datasheet [11]). For the carbon fiber, we used a transverse isotropic model with a longitudinal Young's modulus of 173.24 GPa. Van der Klift et al. [23] found two different experimental values for the longitudinal Young's modulus, 173.24 GPa and 230 GPa, and recommended to use 230 GPa because it corresponds to the TORAYCA® T300 tow made by TORAY®. But we believe that it could be appropriate to retain 173.24 instead of 230 GPa because: 1) it is in the lowest range of Young's modulus for a carbon fiber and a fiber must not be too stiff to be printable; 2) with 173.24 GPa as input, our periodic homogenization model provides a longitudinal Young's modulus very close to 60 GPa for the printed composite material which is consistent with the Markforged Datasheet [11]. Regarding the porosity, we used it as a parameter to fit the experimental data. Figure 2 gives an example of 3 different unit cells with 3 different values of porosity.

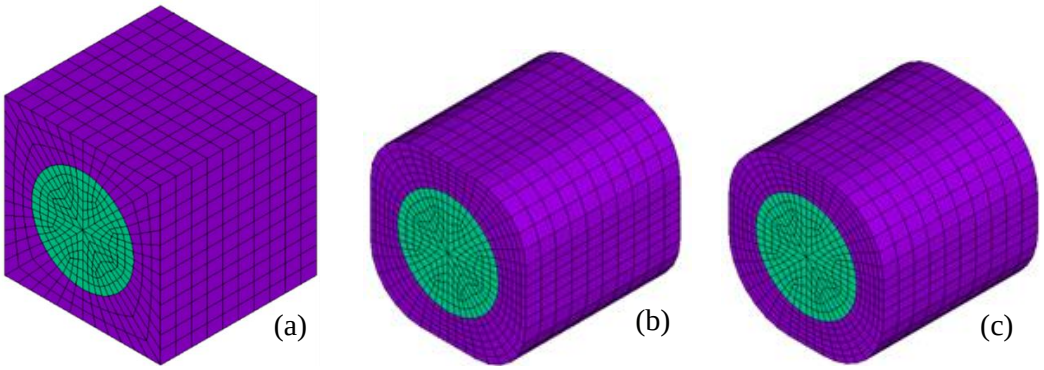

Figure 2 - *Meshes of 3 unit cells with porosity equal to: 0% (a); 9% (b); 13% (c)*

3. VALIDATION OF THE PERIODIC HOMOGENIZATION MODEL

To validate our periodic homogenization model, we compared it to the real material's mechanical behavior in the following way:

- we performed tensile tests on real printed specimens (section 3.1)
- we developed a finite element model of the tensile test by embedding the homogenized properties (section 3.2)
- we compared the numerical results obtained with this FE model to the experimental data (section 3.3).

3.1. Tensile Tests

The tensile tests have been performed on a LR 50K tensile tester produced by Lloyd Instruments (Figure 3). The deformation was measured with an extensometer from Epsilon Technology Corp. The chosen specimen geometry is the ASTM D638-14 Type I, as several articles proved that it was the best geometry to perform tensile tests on 3D printed materials [3, 7, 9, 24, 25]. The parts have been printed with a Markforged X7 printer. The printer imposes a layer height of 0.125 mm for continuous carbon fiber printing. The sample are 26 layers high, with 5 layers of roofs and floors (approximately 0.625 mm) and 2 beads of walls (approximately 0.8 mm). The tensile tests were performed on 3 batches of 5 printed samples:

Figure 3 *- Tensile machine*

- First sample: fibers oriented in the tensile direction (α=0°, Fig. 4b)
- Second sample: fibers oriented perpendicular to the tensile direction (α=90°, Fig. 4c)
- Third sample: fibers oriented with angles of 45° and -45° alternatively (α=45/-45°, Fig. 4d)

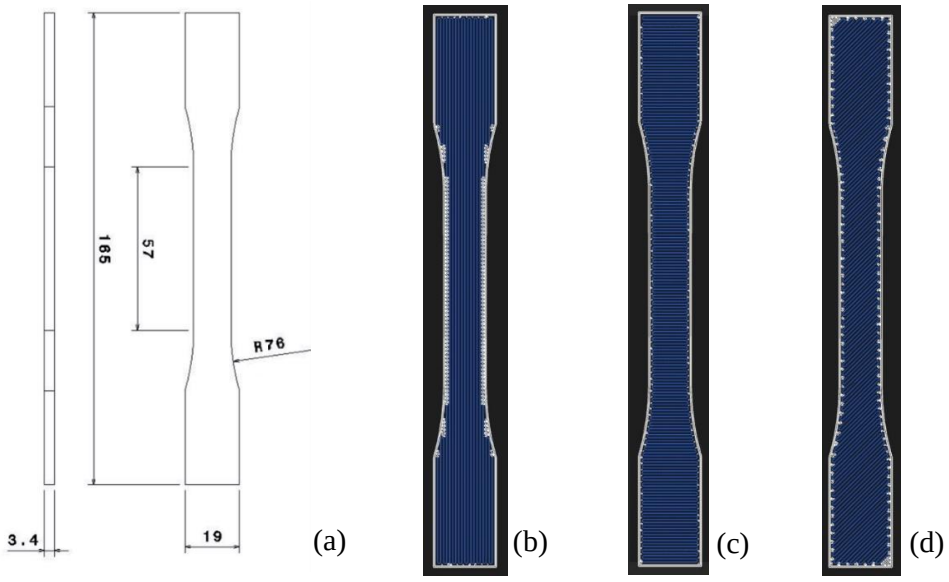

Figure 4 *– Specimen of ASTM D638-14 Type I - (a): dimensions; (b-d): different fibers' orientations*

3.2.Finite Element model

In this section, we present the finite element model of the tensile test we developed with the Ansys mechanical APDL software. The model's geometry is parallelepipedal and the length is equal to the initial length of the extensometer (25 mm). The width and thickness are equal to the mean values of the 5 specimens for each batch. As the printed parts contains walls, roof and floor surrounding the continuous fiber-reinforced material, two different volumes have been defined with two different materials: a composite core and a Nylon envelope, respectively in blue and purple in Figure 5. The composite core was meshed with multilayered SOLSH190 elements while the Nylon envelope was meshed with solid tetrahedrons SOLID186 elements. The two meshed parts were linked with a bonded contact thank to CONTA174 and TARGE170 elements. The behaviors of the walls, floor and roof were modelled with the isotropic properties of the Nylon provided by Markforged [11] while the behavior of the composite was modelled with a linear orthotropic law calculated previously with the periodic homogenization model.

Conventional boundary conditions corresponding to a tensile test were applied by clamping the bottom faces of the structure while the front faces were subjected to a displacement controlling the tensile test along the x-axis.

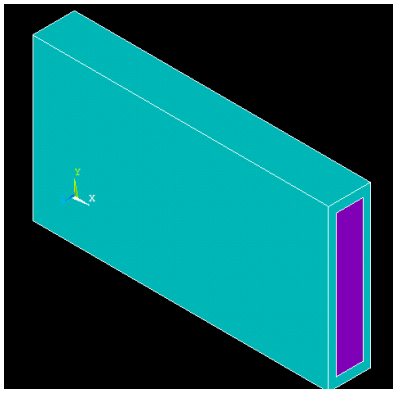

Figure 5 *- FE geometry of specimen (composite material in purple, Nylon in blue)*

3.3.Results and discussion

To assess the appropriateness of the periodic homogenization model including porosity, we compared the experimental data with finite element results, as shown in Figures 6 and 7. Four cases, represented by circles in Figure 6, were studied with a variation of the porosity from 0 to 13% and two intermediate values of 5% and 9%. The Young's Moduli E of the specimen were calculated in each case by dividing the reaction force F (computed on the bottom faces of the specimen with the FE model) by the areas S of these faces multiplied by a strain ε equal to 0.5%:

$$E = \frac{F}{0.005 \times S} \tag{6}$$

In Figure 6, the vertical axis represents the ratio of correlation between two Young's moduli: the first is calculated according to eq. (6) and the second one is measured with the test. The ratio value is closer to 1, and the numerical computation result agrees better with that of experiments. Figure 6 shows that the correlation is almost perfect along the fibers (α=0°). In addition,

in the fiber direction, the porosity has a low influence on the stiffness since the ratio of correlation remains very close to 1 in the four cases. This was expected because the stiffness of the specimen in the longitudinal direction is mainly influenced by the stiffness of the fiber, and it is well known [9] that the porosity is mainly located inside the matrix and not the fiber. On the other hand, we can see that the porosity has a huge influence on the stiffness in other directions (α=90° and α=45°/-45°) and that the stiffness of the model logically decreases when the porosity increases.

In addition, it is observed in Figure 6 that the ratio of correlation for the 45°/-45° sample is better with a low porosity (under 1%). That indicates that the printing process has a huge influence on the void creation within the printed part, and a composite printed with an alternance of layers 45°/-45° is beneficial to decrease the voids content. This property was studied by Rodríguez et al. [26] who proved that each printing pattern resulted in a different porosity.

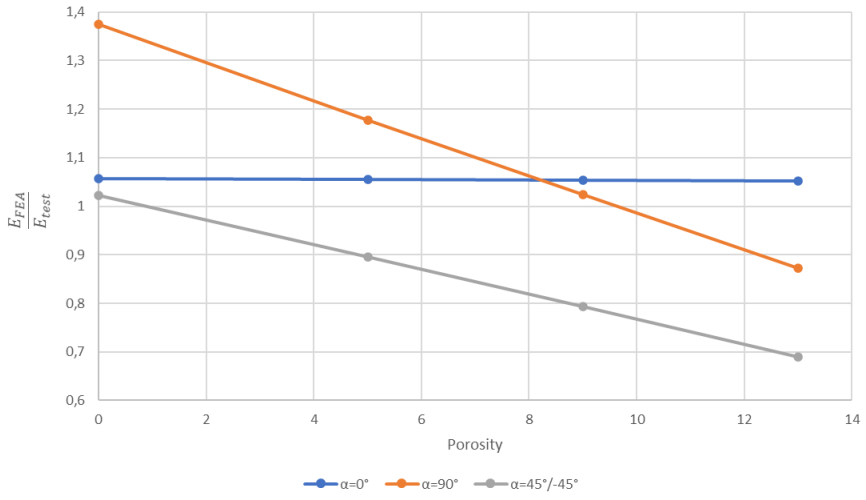

Figure 6 *- Correlation between tensile test and finite element simulation*

Finally, with a porosity around 10%, it is noted in Figure 6 that the ratios of correlation are equal to 1 in the longitudinal as well in the transverse directions. This porosity value corresponds to the measurements performed by Melenka et al. [3], Blok et al. [9] and Ekoi et al. [22], as reported in Table 2. That proves that the periodic homogenization model including the effect

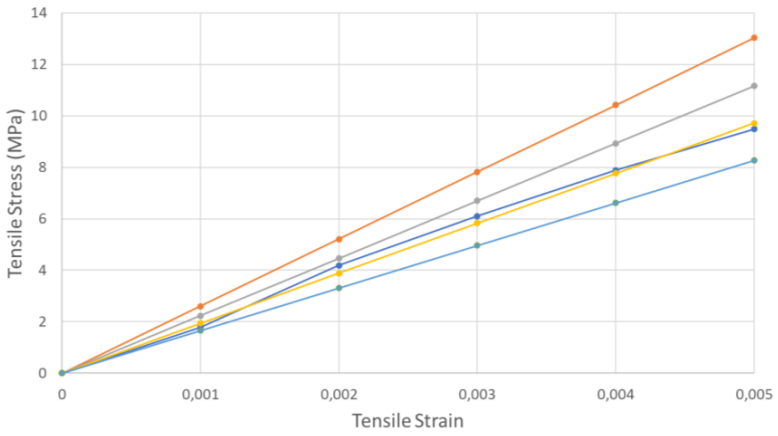

Figure 7 *- Stress-Strain curves (α=90°)*

of the porosity can provide reliable information on the material properties in the direction transverse to the fiber. This is confirmed by Figure 7 where the stress-strain curve computed with a porosity of 9% fits almost perfectly with the stress-strain curve of the test.

4. CONCLUSION

We developed a finite element model including the effect of porosity to predict the material properties of 3D-printed continuous carbon fiber-reinforced composites. This model is based on the periodic homogenization theory and allows to link the properties of the constituents at the microscopic scale with the homogeneous equivalent properties of the printed composite at the macroscopic scale. The reliability of this model was assessed by finding a fair agreement between the numerical results and the experimental data coming from tensile tests performed in 3 different configurations of the fiber's orientation.

The main conclusion is that the porosity has a significant influence on the transverse properties of the printed composite and that the amount of porosity depends on the fiber's orientation difference between two layers. Therefore, the influence of printing parameters and implicit interrelations between printing parameters and the simulation model will be further investigated in the next step. The final objective is to structure some guidelines or a framework to support the development of a new simulation-driven generative design for AM method, which is tailored for this special composite printing process to gain computation cost via the proposed simulation model.

ACKNOWLEDGMENTS

The authors are grateful for the technical support of Rémy Lachat and Christophe Monnot in the use of experimental devices.

REFERENCES

[1] G. Liao, Z. Li, Y. Cheng, D. Xu, D. Zhu, S. Jiang, J. Guo, X. Chen, G. Xu, Y. Zhu (2018). Properties of oriented carbon fiber/polyamide 12 composite parts fabricated by fused deposition modeling. *Materials and Design 139*, 283-292.

[2] N. van de Werken, H. Tekinalp, P. Khanbolouki, S. Ozcan, A. Williams, M. Tehrani (2020). Additively manufactured carbon fiber-reinforced composites: State of the art and perspective. *Additive Manufacturing 31*, 100962.

[3] G.W. Melenka, B.K.O. Cheung, J.S. Schofield, M.R. Dawson, J.P. Carey (2016). Evaluation and prediction of the tensile properties of continuous fiber-reinforced 3D printed structures. *Composite Structures 153*, 866-875.

[4] J. Majko, M. Saga, M. Vasko, M. Handrik, F. Barnik, F. Dorčiak (2019). FEM Analysis of long-fibre composite structures created by 3D printing. *Transport Research Procedia 40*, 792-799.

[5] E. Polyzos, A. Katalagarianakis, D. Polyzos, D. Van Hemelrijck, L. Pyl (2020). A multiscale analytical methodology for the prediction of mechanical properties of 3D-printed materials with continuous fibres. *Additive Manufacturing 36*,101394.

[6] B. Brenken, E. Barocio, A. Favaloro, V. Kunc, R. Byron Pipes (2018). Fused filament fabrication of fiber-reinforced polymers: A review. *Additive Manufacturing 21*, 1-16.

[7] J. Naranjo-Lozada, H. Ahuett-Garza, P. Orta- Castañón, W.M.H Verbeeten, D. Sáiz-González (2019). Tensile properties and failure behavior of chopped and continuous carbon fiber composites produced by additive manufacturing. *Additive Manufacturing 26*, 227-241.

[8] A.U. Aravind, A.R. Bhagat, R. Radhakrishnan (2020). A novel use of twisted continuous carbon fibers in additive manufacturing of composites. *Materials Today: Proceedings*.

[9] L.G. Blok, M.L. Longana, H. Yu, B.K.S. Woods (2018). An investigation into 3D printing of fiber reinforced thermoplastic composites. *Additive Manufacturing 22*, 176-186.

[10] F. Ning, W. Cong, J. Qiu, J. Wei, S. Wang (2015). Additive manufacturing of carbon fiber reinforced thermoplastic composites using fused deposition modeling. *Composites Part B: Engineering 80*, 369-378.

[11] Markforged (2018). Material Datasheet: Composites. https://www-objects.markforged.com/craft/materials/composites-data-sheet.pdf (Accessed: 05/02/2021).

[12] L. Pyl, K. Kalteremidou, D. Van Hemelrijck (2018). Exploration of specimen geometry and tab configuration for tensile testing exploiting the potential of 3D printing freeform shape continuous carbon fibre-reinforced nylon matrix composites. *Polymer Testing 71*, 318-328.

[13] E. Sanchez-Palencia (1979). Non-Homogeneous Media and Vibration Theory. Lecture Notes in Physics. Springer-Verlag, Berlin.

[14] A. Bensoussan, J.L. Lions, G. Papanicolaou (1978). Asymptotic Analysis for Periodic Structures, North-Holland, Amsterdam.

[15] G. Duvaut (1976). Analyse fonctionnelle et mécanique des milieux continus. Applications à l'étude de matériaux composites élastiques à structure périodique. Homogénéisation, in: W.T. Koiter, ed., Theoretical and Applied Mechanics (North-Holland, Amsterdam) 119-132.

[16] G. Duvaut (1984). Homogénéisation matériaux composites. Trends and Applications of Pure Mathematics to Mechanics, Lecture Notes in Physics, 195:35-62.

[17] T.A Dutra, R.T. Luiz Ferreira, H. Borelli Resende, A. Guimarães (2019). Mechanical characterization and asymptotic homogenization of 3D-printed continuous carbon fiber-reinforced thermoplastic. *Journal of the Brazilian Society of Mechanical Sciences and Engineering 41*, 133.

[18] G.-D. Cheng, Y.W. Cai, L. Xu (2013). Novel implementation of homogenization method to predict effective properties of periodic materials. Acta Mechanica Sinica, 29(4):550-556.

[19] T.A. Dutra, R.T. Luiz Ferreira, H. Borelli Resende, A. Guimarães, J. Miranda Guedes (2020). A complete implementation methodology for Asymptotic Homogenization using a finite element commercial software: preprocessing and postprocessing. Composite Structures, 245, 112305.

[20] G. Chabaud, M. Castro, C. Denoual, A. Le Duigou (2019). Hygromechanical properties of 3D printed continuous carbon and glass fibre reinforced polyamide composite for outdoor structural applications. *Additive Manufacturing 26*, 94-105.

[21] R.R. Fernandes, A.Y. Tamijani, M. Al-Haik (2021). Mechanical characterization of additively manufactured fiber-reinforced composites. *Aerospace Science and Technology 113*, 106653.

[22] E.J. Ekoi, A.N. Dickson, D.P. Dowling (2021). Investigating the fatigue and mechanical behaviour of 3D printed woven and nonwoven continuous carbon fibre reinforced polymer (CFRP) composites. *Composites Part B 212*, 108704.

[23] F. van der Klift, Y. Koga, A. Todoroki, M. Ueda, Y. Hirano, R. Matsuzaki (2016). 3D Printing of Continuous Carbon Fibre Reinforced Thermo-Plastic (CFRTP) Tensile Test Specimens. *Open Journal of Composite Materials 6*, 18-27.

[24] R.E. Petruse, S. Pușcașu, A. Pascu, I. Bondrea (2019). Key factors towards a high-quality additive manufacturing process with ABS Material. *Materials Today: Proceedings 12*, 358-366.

[25] J.J. Laureto and J.M. Pearce (2018). Anisotropic mechanical property variance between ASTM D638-14 type i and type iv fused filament fabricated specimens. *Polymer Testing 68*, 294-301.

[26] J.F. Rodríguez, J.P. Thomas, J.E. Renaud (2000). Characterization of the mesostructured of fused-deposition acrylonitrile-butadiene-styrene materials. *Rapid Prototyping Journal*, 6(3) 175-185.